DC/DC Z-SOURCE CONVERTER APPLIED TO PV SYSTEM

DE CASTRO, Lino A.[1], ANTUNES, Fernando L. M.[1] and SÁ, Edilson M.[2]
[1] Federal University of Ceará (UFC)
Electrical Engineering Department
Campus do Pici - 60.455-760 Fortaleza/CE (Brazil).
Phone:+5585 336 69586, e-mail: castro.lac@live.com, fantunes@dee.ufc.br
[2] Federal Institute of Education, Science and Technology of Ceará (IFCE)
Phone:+5585 329 26101, e-mail: edilson.mineiro@gmail.com

Abstract- paper proposes application of a DC/DC Z-Source Converter (ZSC) based on the one-port impedance network, operating in continuous conduction mode (CCM) for solar power generation in DC microgrid. A photovolaic array is connected to the input of ZSC, which provides voltage gain from 167V. The nominal input power of arrangement was 1440 Watts**.**

Attending the low efficiency of photovoltaic modules (PV) and influence suffering by atmospheric conditions two maximum power point tracking techniques (MPPT) were tested to track the maximum power point at any time: Perturb and Observe (P&O) and Incremental Conductance (IC). By PSIM software, the operation of ZSC and MPPT behavior were simulated and prototype experimental results are provided to verify the validity of the converter and each MPPT implemented.

Keywords: Power Electronics, DC / DC Z-Source converter, MPPT, Photovoltaic Systems;

NOMENCLATURE

CCM -Continuous Conduction Mode
DC -Direct Current.
DCM -Discontinuous Conduction Mode
IC - Incremental Conductance
MPPT -Maximum Power Point Tracking
P&O -Perturb and Observe
PV -Photovoltaic.
PWM -Pulse Width Modulated
ZSC -Z-Source Converter

1. INTRODUCTION

As energy demand continues to increase, efforts are being made towards new energy sources and also towards increasing energy output from existing ones. Solar energy is considered to be one of the most reliable and promising source of renewable energy [1].

DC microgrid has many advantages over AC microgrid because it needs only few power converters with higher system efficiency and easier interface of renewable energy sources to DC System[2].Many researches describing different topology of DC/DC ZSC have been presented [3][4][5]. A modified DC/DC ZSC that is based on the one-port impedance network was presented in [5]. The DC/DC ZSC topology with network impedance of a port, besides the simplicity presents greater static gain and less voltage stresses across the capacitors of the z-source network, combined with the ability to operate with high load resistance.

2. CONVERTER TOPOLOGY

The DC/DC ZSC based on the one-port impedance network i consists of an input voltage source V_i, one-port impedance network, two diodes (D_1 and D_2), a switch *S* (IGBT*)*, an output filter capacitor C_O and a load R_O. The one-port impedance network is consisted of two identical capacitors (C_1=C_2), diode D_1 and two identical inductors ($L_1 = L_2$). The one-port impedance network is in series with the input voltage source, thus the input voltage can share the common ground with the output. Basic circuit of the dc/dc Z-source converter is shown in Figure 1. Due to the symmetry of the one-port impedance network($C_1 = C_2$ and $L_1 = L_2$), we have

$$I_{L1} = I_{L2} = I_L,\ V_{L1} = V_{L2} = V_L. \quad (1)$$

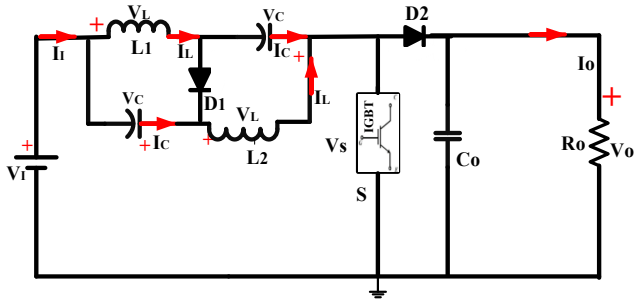

Figure.1-Proposal DC/DC ZSC circuit.

The ZSC has three operating steps, Figure **2(a)** shows the Step 1 .

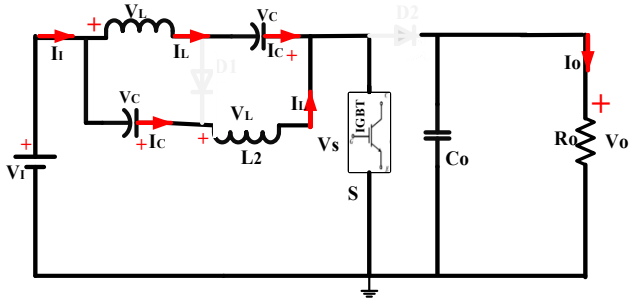

Figure 2(a) -ZSC circuit in Step1 [t_0 t_1].

In this step1, the switch S get forward biased and the diodes are reverse biased, and then the inductors (L_1 and L_2)

978-1-5090-5339-1/17/$31.00 ©2017 IEEE.

capacitors (C_1 and C_2) are supplied by the input voltage (V_I). Figure 2(a) illustrates the ZSC in operation in step 1.
The inductors current begins to rise linearly and reaches to the maximum until the switch is turned off. Assuming,

$$T_{on} = DT_s \quad (2)$$

the current increment $\Delta iL+$ can be expressed as

$$I_L(t) = -I_C(t) \quad (3)$$

$$I_I(t) = 2V_L(t) \quad (4)$$

The voltage relation on the network inductors and the switch is given by equations (3.4) and (3.5) respectively.

$$V_L(t) = V_I(t) + V_C(t) \quad (5)$$

$$V_S(t) = V_I(t) + 2V_C(t) \quad (6)$$

The steps 2 and 3 occurs when the switch S is turned off as shown in Figures 2(b) and 2(c) respectively.

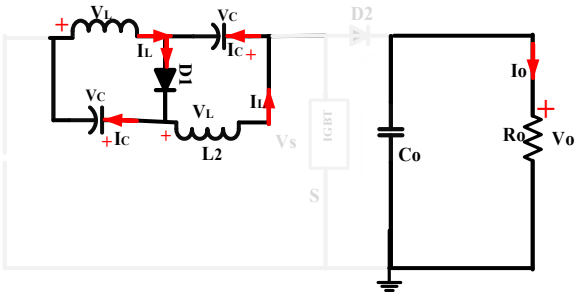

Figure 2(b) -ZSC circuit in Step2 [$\mathbf{t_1\ t_2}$].

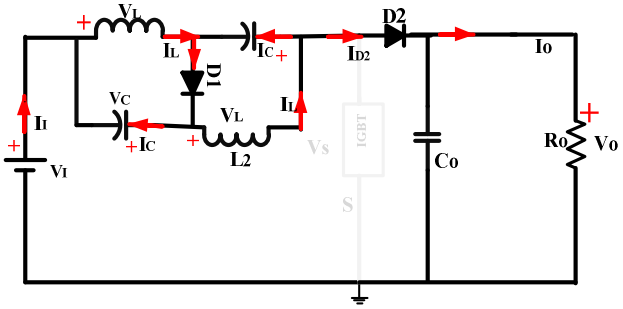

Figure 2(c) -ZSC circuit in Step2 [$\mathbf{t_2\ t_3}$].

In Step2 the switch S and D_2 are turned off and diode (D_1) is forward biased in this the interval. As the inductors L_1 and L_2 charge the capacitors C_1 and C_2, the inductor current I_L is decreasing linearly and the one-port impedance network is isolated from both the input voltage V_I and the load R_0. Once the voltage V_S increases to be greater than V_0, diode D_2 get forward biased, Step2 will end. The Electrical current relationship is given by equations (7) and (8) respectively.

$$I_{L1}(t) = -I_C(t) \quad (7)$$

$$I_{D1}(t) = 2L(t) \quad (8)$$

The voltage on the switch S

$$V_S(t) = V_I(t) + 2V_C(t) \quad (9)$$

In this step, the switch S is still reverse biased, while $\mathbf{D_1}$ and $\mathbf{D_2}$ diodes conduct simultaneously. Thus, equation (11) result from established equation (10).

$$I_I(t) = I_L(t) - I_C(t) \quad (10)$$

$$I_{D1}(t) = 2I_L(t) - I_I(t) \quad (11)$$

The one-port impedance network inductors charge the capacitors (C_1 and C_2) and supply the output capacitor C_0 and load R_0 with the input voltage input V_I. The inductor current I_L decrease linearly and Step 3 ends when switch S get forward biased again in the following switching period. Thus, the duration time of steps 2 and 3 is $T_{off} = (1 - D)T_s$.

.

2.1. BOOST FACTOR CALCULATION

Due to the high capacitance of the z-source network and the high switching frequency, the capacitors voltage (V_C) is nearly constant. Considering inductors voltage of the z-source network (V_L) is equal $V_I + V_C$ during the conduction of the switch S and equal $-V_C$ when switch S is turned off. Thus, it follows the equation (12).

$$(V_I + V_C).D.T_s + (-V_C)(1 - D).T_s = 0 \quad (12)$$

From equation (12), result the capacitor voltage V_C expression (13):

$$V_C = \frac{D.V_I}{1-2D} \quad (13)$$

From (12) e (13), ignoring the diode voltage drop we have the voltage gain G_V , given by

$$G_V = \frac{V_o}{V_I} = \frac{1}{1-2D} \quad (14)$$

Where

V_o -output voltage; V_I- input voltage and D- duty cycle.

Figure 3 illustrates the output voltage curves as a function of the duty cycle (D) and input voltage (V_I).

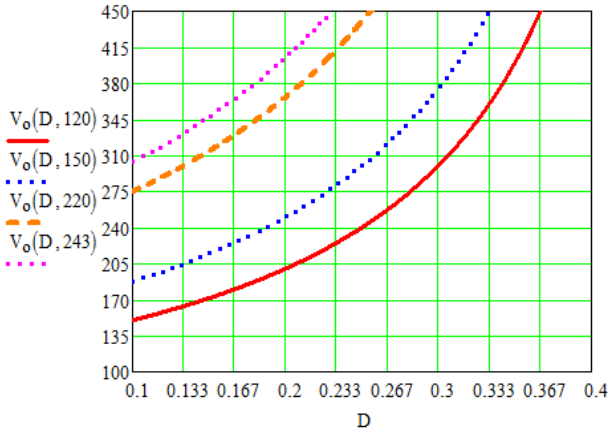

Figure 3- output voltage curves as a function of the D and V_I.

3. PROJECT SPECIFICATIONS

The ZSC can operate in three different modes:

- $\frac{1}{2}\Delta I_L < I_I$: Continuous Conduction Mode (CCM)
- $\frac{1}{2}\Delta I_L = I_I$: Critical Conduction Mode (CritCM)
- $\frac{1}{2}\Delta I_L > I_I$: Discontinuous Conduction Mod (DCM)

To ensure that the ZSC operates in CCM, the inductor current must be greater than zero during the entire switching period.

3.1. Minimum Inductance And Capacitance in CCM

$$L_{min} \geq \frac{(1-D)(1-2D)D.R_o}{x_L.f_s} \qquad (15)$$

Where:
x_L is the current ripple ΔI_L adopted on the project to z-network inductors. In CCM, the value x_L is between 15% and 25% of the I_L current [5].

$$C_{min} = \frac{D.I_L}{x_C.V_C} = \frac{(1-2).I_L}{x_C.V_I.f_s} \qquad (16)$$

Where:
x_C is the voltage ripple ΔV_C adopted on the project to z-network capacitors.

In this work the z-network inductors and capacitors calculated were $2x10^{-3}$ Henry ($L_1 = L_2$) and $150x10^{-6}$ Farad ($C_1 = C_2$), respectively. Table 1 shows some parameters values of DC/DC ZSC in CCM.

Table 1- Project Specifications

Parameters and components	Codes / Values
IGBT Switch	**IRGP50B60PD**
Diodes	**HFA25PB60**
Nominal Power of PV Arrangement (P_I)	$P_I = 6x240 = 1,4\ kW$
Ripple current in the z-network inductors (ΔI_L)	**24%**
Nominal output Power (P_o)	$P_o = P_I \times \eta = 1,38\ kW$
Nominal output current (I_o)	$I_o = \frac{P_o}{V_o} = 3,45\ A$
Maximum power point voltage (V_{PV})	$V_{PV} = 6x40,5 = 243\ V$
Output Voltage (V_o)	$400V$
Switching frequency (F_s)	$40kHz$
Output Voltage Ripple (ΔV_o)	**2%**
Output Current Ripple (ΔI_o)	**10%**
Nominal Load Resistance (R_o)	$R_o = \frac{V_o^2}{P_o} = 120\Omega$

4. MPPT CONTROL TECHNIQUES

The main disadvantage of PV panel is the low efficiency of energy conversion as compared with other alternative resources. PV is a non-linear source that depends on irradiation and temperature in its operation [6]. The photovoltaic module operation depends strongly on the load characteristics to which it is connected, as shown in [7]. To overcome this problem, it is necessary to add an adaptation device, an MPPT controller with a DC/DC converter, between the source and the load. Figure 4 shows the Proposed PV System Power Flow. Due to variations in solar insolation temperature, PV systems do not continually deliver their theoretical power unless a MPPT is used [8].

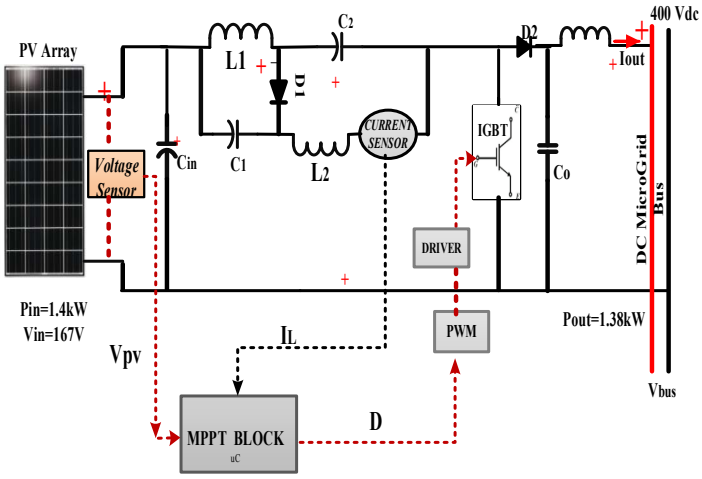

Figure. 4.- Proposed PV system Power Flow.

Therefore, two types of MPPT control techniques and constant voltage control on DC microgrid bus are implemented. The last technique is to regulate the output current and DC bus voltage. The MPPT control techniques tested are: *Perturb and Observe (P&O) and Incremental Conductance (IC)*. Figure 5 shows how the controllers generate a perturbation by decreasing or increasing the PWM duty cycle and observing its effect on the output PV power.

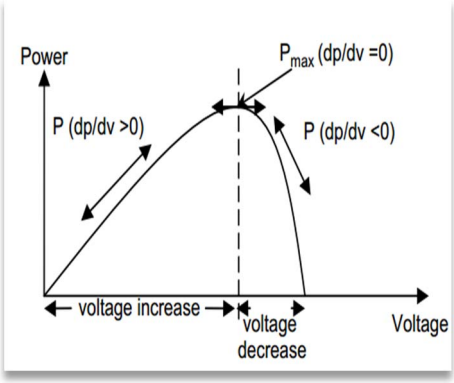

Figure.5-PxV Characteristic of a PV module.

4.1. *Perturb and Observe (P&O)*

P&O method operates periodically incrementing or decrementing the output terminal voltage PV and comparing the power obtained in the current cycle with the power of the previous cycle. If the voltage and varies the power increase, the control system switches the operation point in that direction; otherwise changes the operating point in the opposite direction. This method is considered the standard to obtain high efficiency. The flowchart 6 describes the P& O algorithm.

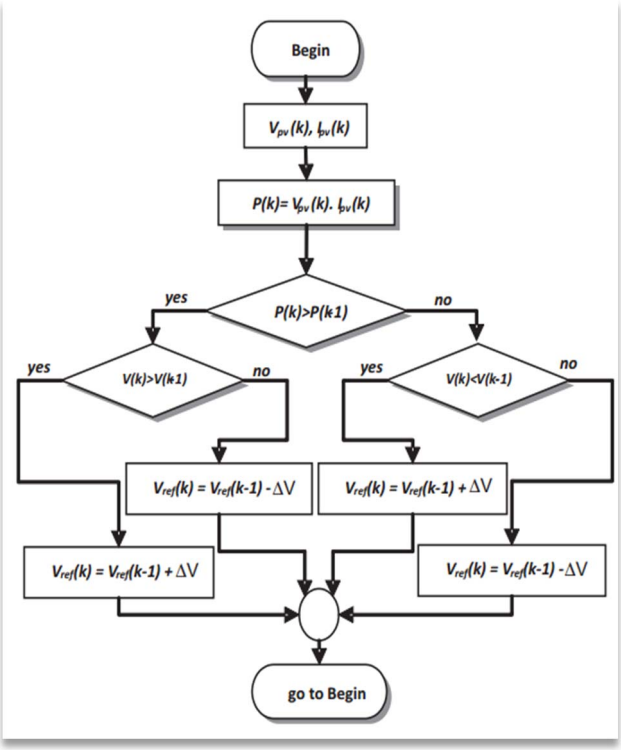

Figure 6 - P&O MPPT Technique Flowchart.

If the instant power P(k) is greater than the previous computed power P(k-1), then the direction of perturbation is maintained otherwise it is reversed.

- When $dP/dV > 0$, the voltage is increased, this is done through: $\mathrm{D(k)} = \mathrm{D(k-1)} - \Delta\mathrm{V}$
  .
- When $dP/dV < 0$, the voltage is decreased through $\mathrm{D(k)} = \mathrm{D(k-1)} - \Delta\mathrm{V}$

4.2. Incremental Conductance (IC)

This method is based on the values of the instantaneous and incremental conductance of the PV array. These quantities are obtained by the current and voltage measurements of the PV array. The derivative of the PV power in relation to the voltage can be written as follows:

$$\frac{\mathrm{dP}}{\mathrm{dV}} = \frac{\mathrm{d(V \times I)}}{\mathrm{dV}} = \mathrm{I} + \mathrm{V} \times \frac{\mathrm{dI}}{\mathrm{dV}} \qquad (17)$$

Dividing each member of equation (17) by V, result:

$$\frac{1}{\mathrm{V}} \times \frac{\mathrm{dP}}{\mathrm{dV}} = \frac{\mathrm{I}}{\mathrm{V}} + \mathrm{V} \times \frac{\mathrm{dI}}{\mathrm{dV}} \qquad (18)$$

Due to measurement noise, quantization errors and, in particular, the reference voltage discretization. Therefore, it is necessary to define a tolerable band (ΔW) around zero where such a condition can be considered true:

$$-\Delta\mathrm{W}/2 < \mathrm{I/V} + \mathrm{dI/dV} < \Delta\mathrm{W}/2 \qquad (19)$$

And thus the technique is given the flowchart of Figure 7.

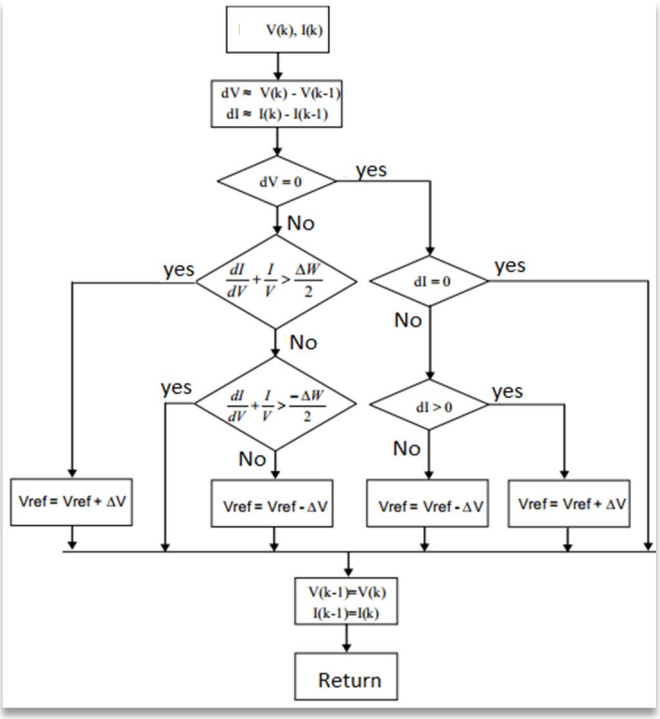

Figure.7– IC MPPT Technique Flowchart.

5. Simulation and Experimental Results

5.1. Simulation Results

First, the ZSC circuit was simulated without the MPPTs in the PSIM 9.1 software and in the Figure 8 is shown the simulated current $\mathrm{I_{D1}}$ and voltage $\mathrm{V_{D1}}$ in the diode $\mathrm{D_1}$. Figure 9 shows the simulated Inductor current $\mathrm{I_L}$ and voltage $\mathrm{V_c}$ in the z-network.

In the next step, was simulated end tested the two the MPPT techniques, for example Figures 10 shows the effect of temperature, which changed from $40^{\mathrm{o}}\,\mathrm{C}$ to $25^{\mathrm{o}}\,\mathrm{C}$, while the irradiance (G) was constant $(1000\,W/m^2)$ using P&O. Figure 11 shows the irradiance effect on the system. The irradiance changed from $1000\,W/m^2$ to $800\,W/m^2$, while the temperature was kept constant $(25^{\mathrm{o}}\,\mathrm{C})$ The principal parameters are: Input Power (P_{max}) , output power (P_O); PV array voltage (V_{PV}); Output power (V_O); Output Current (I_O); Temperature (T_{emp}); Irradiance (G).

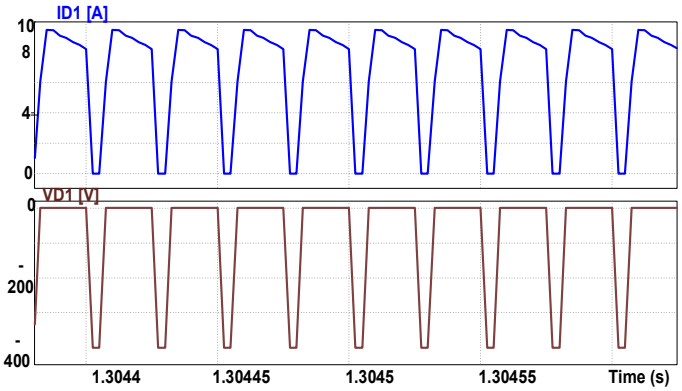

Figure 8-Simulated current in the diode D_1.

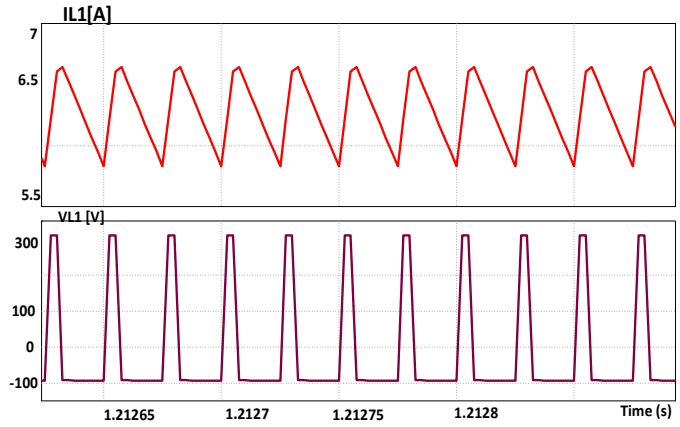

Figure 9- Simulated Inductor current I_L in the z-network.

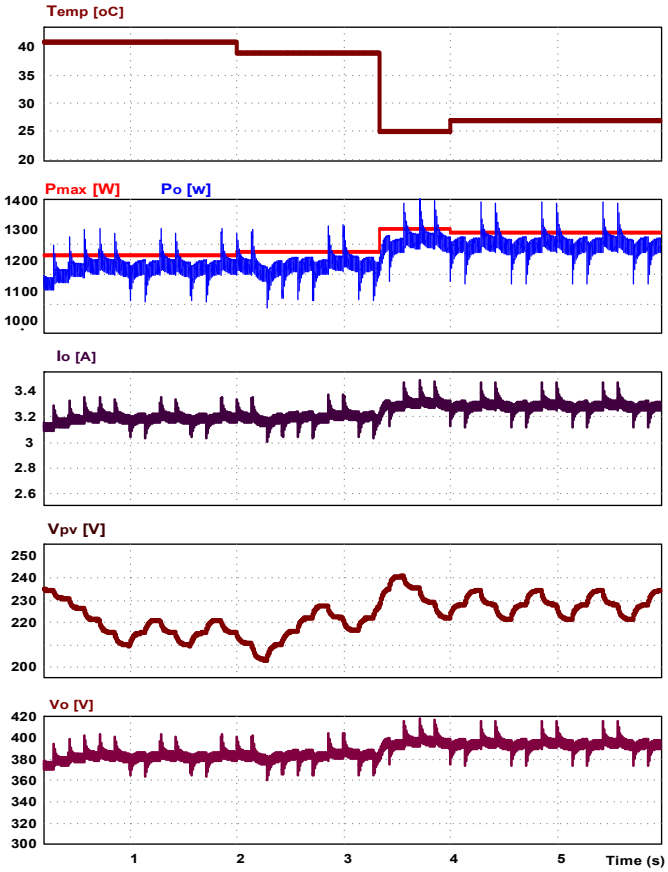

Figure 10- effect of temperature, which changed from 40^{o} C to 25^{o} C, while the irradiance (G) was constant .

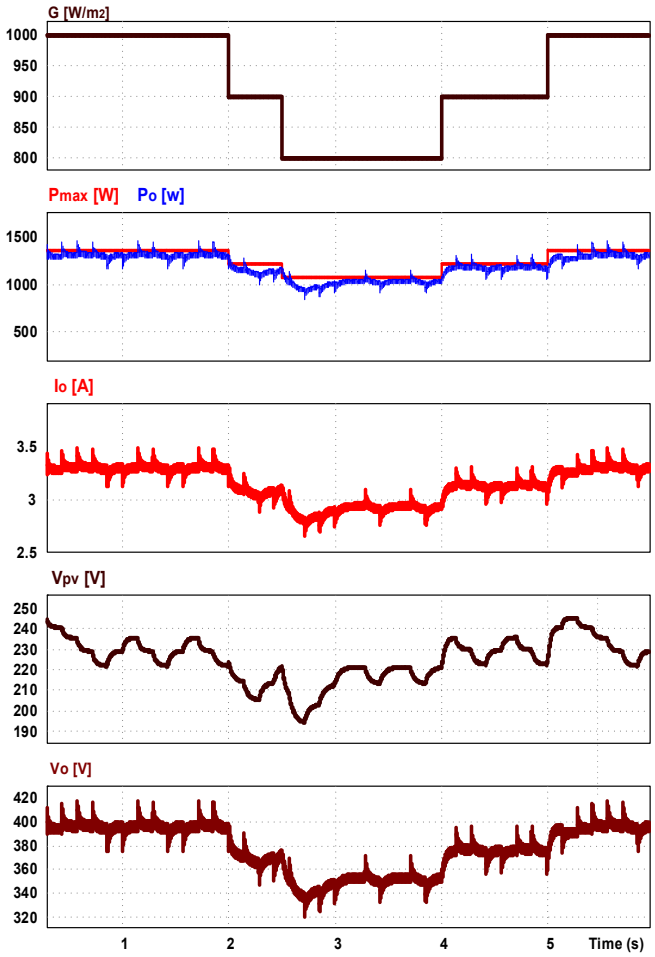

Figure 11- effect of irradiance, which changed 1000 W/m^2 to 800 W/m^2, while the temperature was constant .

5.1. Experimental Results

The prototype was implemented (Figure 14) and results wave forms of current and voltage in the diode D_1 are shown in Figure 12. Figure 13 shows the obtained wave forms of current I_L and voltage V_c on the prototype. The theoretical value are similar to the practical values.

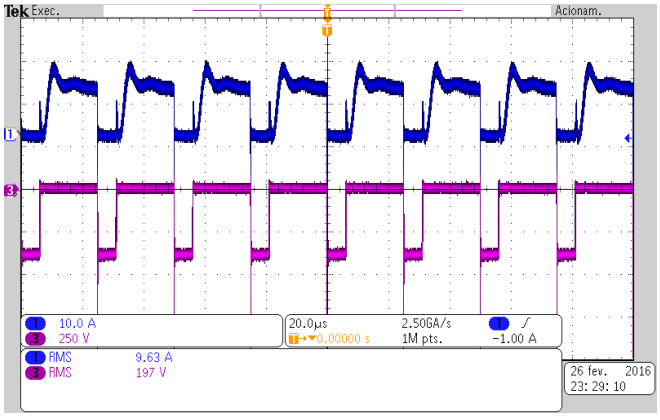

Figure.12-Prototype current in the diode D_1.

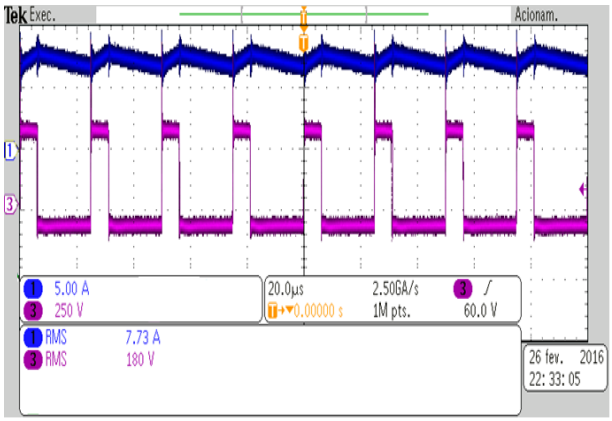

Figure 13-Prototype current I_L in the z-network.

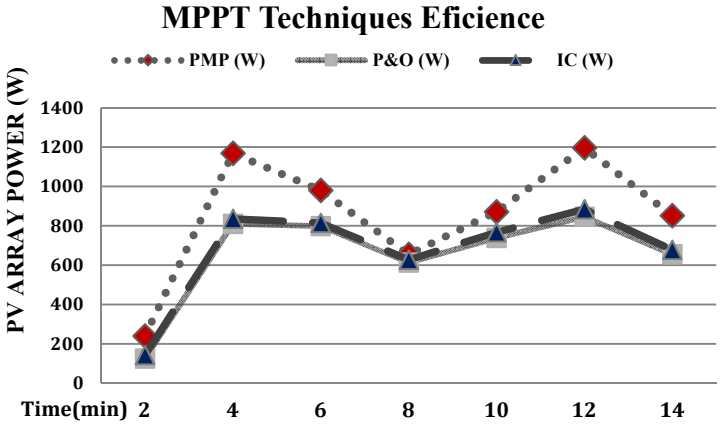

After evaluated the prototype efficiency of Two MPPT techniques were compared, P&O and IC. Figure 15 shows the P&O and IC results. The MPPT techniques average efficiencies were 79.9% and 82.5% respectively.

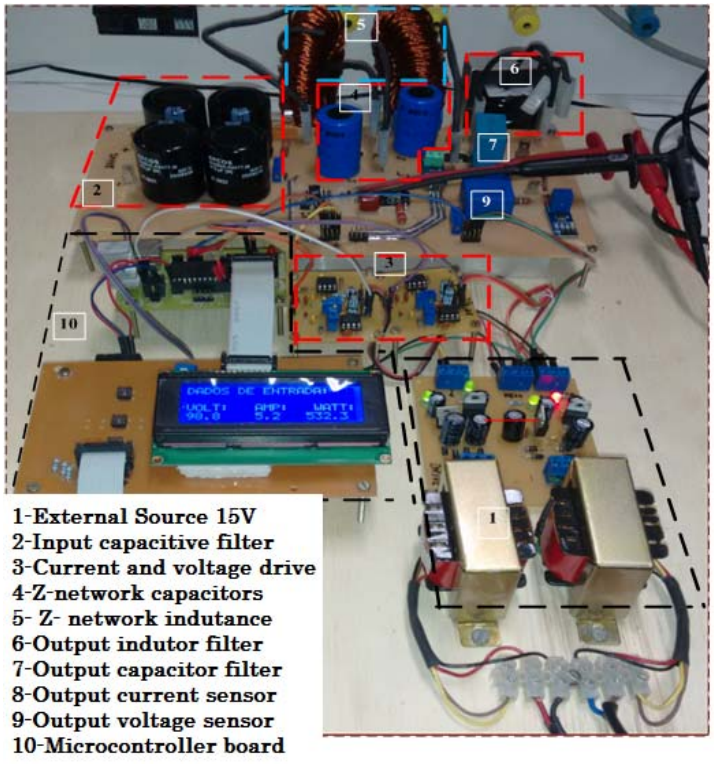

Figure 14- Prototype of the ZSC converter.

6. CONCLUSIONS

This work aimed to develop a high gain DC/DC converter applied to a photovoltaic system. The simulation and prototype of a DC/DC ZSC were presented.

After evaluated the prototype efficiency of Two MPPT techniques were compared, P&O and IC. The MPPT techniques average efficiencies were 79.9% and 82.5% respectively. In the P&O technique, the disturbance occurs periodically over the voltage or current of the PV module by varying the duty cycle of a DC / DC converter. This situation causes that even in the point of maximum power it continues oscillating, whereas in the technique IC after finding the point of maximum power tends not to oscillate avoiding losses that occur in P&O. From DC Bus it's possible supply power to the users with different type of load systems are interconnected, without inverter for DC devices or with inverter for AC small devices.

7. FUTURE WORK

The model of the ZSC using digital controller can be designed which may give more freedom to chose best compensator parameters and compare system performance using other MPPT techniques like fuzzy logic control and implantation of adaptive control architecture for MPPT can be used to supply the loads under changes of the solar insolation and ambient temperature.

To develop control strategies for DC bus and using film capacitors for reducing EMI in order increase the efficiency of topology.

ACKNOLEDGEMENTS

This article would like to thank the Group of Energy Processing and Control (GPEC), Federal University of Ceará (UFC) by the structure provided to conduct this work and the Coordination of Improvement of Higher Education Personnel (CAPES) for financial support to this project.

REFERENCES

[1]. P. Bhatnagar, R.K. Nema "Maximum power point tracking control techniques: State-of-the-art in photovoltaic applications" Renew Sustain Energy Rev, 23 (2013), pp. 224–241.

[2].Zhi Na, Zhang Hui And Xing Xiaowen "Power Control Of DC Microgrid With Variable Generation And Energy Storage" International Journal OfAutomation And Power Engineering(IJAPE) Volume 2 Issue 4, May 2013.

[3].PENG, Fang Z, Z-Source Networks for Power Conversion, Applied Power Electronics Conference and Exposition, APEC. Twenty-Third Annual IEEE, 2008.

[4].GALIGEKERE, Veda Prakash and KAZIMIERCZUK, Marian K., Fellow, IEEE, "Analysis of PWM Z-Source DC-DC Converter in CCM for Steady state",IEEE Transaction on Circuits and Systems-I: Regular Paper,vol.59,no.4,pp.854-863,April-2012

.

[5].LIQIANG Yang et all, "A Modified Z-Source DC-DC Converter", School of Electric Power, South China University of Technology IEEE Power Electronics and Applications (EPE'14-ECCE Europe), 2014 16th European Conference on

[6]. R. Khanna, Q. Zhang, W. E. Stanchina, G. F. Reed, and Z.-H. Mao,"Maximum power point tracking using model reference adaptive control,"IEEE Trans. Power Electron., vol. 29, no. 3, pp. 1490–1499, Mar. 2014.

[7]. C. Larbes , S. M. A. Cheikh , T. Obeidi and A. Zerguerras "Genetic algorithm optimizedfuzzy logic control for the maximum power point tracking in photovoltaic system", *Renew. Energy*, vol. 34, no. 10, pp.2093 -2100 2009.

[8].M. Mohd Zainuri, M. Mohd Radzi, A. Soh, and N. Rahim, "Development of adaptive perturb and observe-fuzzy control maximum power pointtracking for photovoltaic boost dc-dc converter,"IET Renew. Power Gen.vol. 8, no. 2, pp. 183–194, Mar. 2014.